ELSEVIER

Chemical Geology 227 (2006) 70–82

CHEMICAL GEOLOGY
INCLUDING
ISOTOPE GEOSCIENCE

www.elsevier.com/locate/chemgeo

Water diffusion in basaltic to dacitic glasses

Satoshi Okumura [a,*], Satoru Nakashima [a,b]

[a] Department of Earth and Planetary Sciences, Tokyo Institute of Technology, Tokyo 152-8551, Japan
[b] Interactive Research Center of Science, Tokyo Institute of Technology, Tokyo 152-8551, Japan

Received 26 October 2004; received in revised form 28 September 2005; accepted 30 September 2005

Abstract

Dehydration experiments on basaltic, andesitic and dacitic glasses with 1.1, 0.7 and 1.0 wt.% total water, respectively, were performed at 400–675 °C and 0.1 MPa. The dehydration rates were measured by in situ infrared (IR) spectroscopy and modeled by assuming the diffusion of one component water (total water). The diffusivities of total water in basalt and dacite were found to be linearly dependent on total water contents, but that in andesite was weakly dependent on or independent of total water contents at water content and temperature ranges of this study. The total water diffusivities in basalt and dacite were determined by assuming the linear-dependent diffusivity on total water contents and that in andesite was obtained by assuming the constant diffusivity. The obtained diffusivities of total water D ($\mu m^2/s$) can be expressed by the following equations:

$$D_{\mathrm{Basalt}} = C/C_0 \exp[(20.2 \pm 2.1) - (166,000 \pm 13,000)/RT]$$

$$D_{\mathrm{Andesite}} = \exp[(12.4 \pm 1.4) - (138,000 \pm 10,000)/RT]$$

$$D_{\mathrm{Dacite}} = C/C_0 \exp[(13.9 \pm 0.9) - (133,000 \pm 6000)/RT],$$

where C is the total water contents in weight percent; C_0, reference total water contents of 1.1 and 1.0 wt.% for basalt and dacite, respectively; and T, temperature in Kelvin. These equations cover the temperature ranges of 400–575, 500–675 and 500–675 °C, and the water content ranges of <1.1, 0.7 and 1.0 wt.% for basalt, andesite and dacite, respectively. The obtained diffusivities of total water in basalt, andesite and dacite and previous data for water diffusivity in rhyolite show that at 0.7 wt.% and 400–675 °C, the total water diffusivity decreases from rhyolite to andesite, but the total diffusivity in basalt is higher than that in dacite and lower than that in rhyolite. On the other hand, the results of this study predict that the diffusivities of total water in basalt to rhyolite increase with depolymerization of silicate structures at higher temperatures, which results from the crossovers of diffusivity–temperature trends.

Keywords: Water diffusivity; Basalt; Andesite; Dacite; Infrared spectroscopy

1. Introduction

Determination of water diffusivity in silicate melts and glasses is important in understanding and modeling magma ascent processes during volcanic eruptions, because the water diffusivity controls the rates of bub-

* Corresponding author. Present address: Department of Earth and Space Science, Osaka University, Machikaneyama-cho 1-1, Toyonaka-shi, Osaka 560-0043, Japan. Tel.: +81 6 6850 5559.
E-mail address: sokumura@ess.sci.osaka-u.ac.jp (S. Okumura).

0009-2541/$ - see front matter © 2005 Elsevier B.V. All rights reserved.
doi:10.1016/j.chemgeo.2005.09.009

ble nucleation and growth during magma ascent (e.g., Sparks et al., 1994; Toramaru, 1995; Liu and Zhang, 2000). Diffusive transport of water to the bubbles causes the variation of physical properties (viscosity and density) of magmas, because the physical properties are dependent on the water content (e.g., Hess and Dingwell, 1996; Ochs and Lange, 1999). Variation of water contents is also influential in the dynamics of magma flow in the volcanic conduit (Melnik and Sparks, 1999) and the bubble formation process (Lensky et al., 2001).

There are many published data of the water diffusivity in rhyolitic melts and glasses which cover wide ranges of temperatures, pressures and total water contents (e.g., Shaw, 1974; Delaney and Karsten, 1981; Karsten et al., 1982; Lapham et al., 1984; Zhang et al., 1991a; Jambon et al., 1992; Zhang and Behrens, 2000). Zhang et al. (1991a) determined the water diffusivity in rhyolitic glasses by taking into account the water speciation (hydroxyl groups and molecular water). Their results indicated that only molecular water was the diffusive species, and that at a given temperature, the diffusivity of molecular water can be considered as a constant at water contents of <1.7 wt.%. Nowak and Behrens (1997) found that total water diffusivity in haplogranitic melt was linearly dependent on water contents at <3 wt.% and exponentially at >3 wt.%. This change from linear to exponential concentration-dependence may be attributed to the modification of melt structure by incorporation of hydroxyl groups (Behrens and Nowak, 1997). Zhang and Behrens (2000) presented formulations to describe water diffusivity in rhyolitic melts and glasses which covered the wide ranges of temperature (400–1200 °C), pressure (0.1–810 MPa) and water contents (0.1–7.7 wt.%). In the determination of water diffusivity, they assumed that the diffusivity of molecular water was exponentially dependent on water contents for explaining the exponential dependence of total water diffusivity on water contents. This assumption was supported by the following two arguments. First, the experimental results could be well reproduced by modeling with exponential dependence of molecular water diffusivity on water contents, and second the diffusivity of argon (molecular species) in silicate melts showed the exponential dependence on water contents (Behrens and Zhang, 2001). These results for the water diffusivity in rhyolitic melts and glasses are applicable to model the bubble formation processes and the dynamics of magma flow in rhyolitic volcanic eruptions.

On the other hand, only a few experimental studies have been performed to determine the water diffusivity in other natural composition glasses and melts (Zhang and Stolper, 1991; Behrens et al., 2004; Liu et al., 2004). Zhang and Stolper (1991) determined the total water diffusivity in basaltic melts with <0.43 wt.% water at 1300–1500 °C and 1 GPa. The water content profiles obtained after diffusion–couple experiments were successfully reproduced by the model of molecular water diffusion and equilibrium water speciation, which might suggest that molecular water was the diffusive species for water diffusion in basaltic melts as well as in rhyolitic melts and glasses. The obtained diffusivities of total water in basaltic melts were linearly dependent on total water contents and were 30–50 times larger than those in rhyolitic melts. Recently, Behrens et al. (2004) investigated the water diffusivity in andesitic and dacitic melts at 1185–1585 °C and 0.5–1.5 GPa. They showed that total water diffusivity in dacitic melts was proportional to water contents as well as those in basaltic and rhyolitic melts. The diffusivity of total water in andesitic melts was also dependent on water contents, but the dependence was weaker than that for dacite. In addition, Behrens et al. (2004) found that the water diffusivities in silicate melts increased with melt depolymerization at temperatures above 1200 °C by combining their results with previous studies on basaltic and rhyolitic melts. These water diffusivities in basaltic to dacitic melts at higher temperatures and pressures are applicable to deep magmatic processes.

The water diffusivities in basaltic to dacitic melts and glasses at lower temperatures and pressures are also essential to discuss shallow magmatic process. Liu et al. (2004) performed the dehydration experiments at 551–637 °C and 0.1–145 MPa to determine the water diffusivity in dacitic melts. The obtained diffusivity of total water depended on total water contents and was smaller than water diffusivity in rhyolitic melts, whereas water diffusivity in dacitic melts was larger than that in rhyolitic melts at higher temperatures (Behrens et al., 2004). Liu et al. (2004) suggested that the mobility of water appeared to be reduced by introducing alkaline earth elements in the melts at low temperatures. However, the experimental data of the water diffusivities in natural composition melts and glasses are not enough to discuss the diffusion process in those melts and glasses. This study presents new data sets of the water diffusivities in basaltic, andesitic and dacitic glasses at 400–675 °C and 0.1 MPa. The present data are relevant to water behavior in magma at shallow depth, and effects of melt and glass compositions on water diffusion are discussed.

2. Experimental methods

2.1. Starting materials

We prepared hydrous glasses with basaltic, andesitic and dacitic compositions. The basaltic glass is a natural sample from South Arch volcano. This sample was collected at 250 km southern sea floor from Hawaii Island during the 697th dive of the JAMSTEC (Japan Marine Science and Technology Center) submersible *Shinkai 6500* in 2001. The chemical compositions of the basaltic glass were analyzed with a JEOL-JXA-8800 electron microprobe using a defocused beam (10 μm in diameter), 15 kV accelerating voltage, and 12 nA beam current. The analytical results are listed in Table 1. The water content in the doubly polished basaltic glass was determined from peak intensities at 3550 cm^{-1} in the transmitted infrared (IR) spectra obtained by FT-IR microspectrometer (Jasco IRT30 + FTIR-620 Plus). The sample thickness determined by a laser scanning confocal microscope (LSCM) (KEYENCE, Color Laser 3D Profile Microscope VK-8500 and VK-8510) and the molar absorptivity of 64 L/mol cm (Yamashita et al., 1997) were used to calculate the water content. The water content of the basaltic glass was determined to be 1.1 wt.%.

Andesitic and dacitic glasses were synthesized from natural pumices of the 1975 and 1914 eruptions at Sakurajima Volcano, Japan, respectively. The andesitic and dacitic glasses were made by melting experiments at high pressure and temperature (high *P–T*) which were performed using an internally heated pressure vessel (IHPV: SMC2000). The powdered samples of the pumices were introduced into $Au_{75}Pd_{25}$ capsules (5 mmϕ), then the capsules were sealed. The high *P–T* experiments were performed at 1300 °C and 100 MPa for 10 h. After the experiments, the capsules were opened and the glass samples were examined under an optical microscope. No crystals were observed in the samples, but a small number of bubbles were found. These bubbles, which are often observed when melting experiments are conducted for powder samples, might be made from extra N_2 gas in the air entrapped in the sealed capsules. The glass parts without bubbles are used in the following dehydration experiments.

Table 1
Chemical compositions, water contents and NBO/T of the samples

	Basalt	Andesite	Dacite
SiO_2	46.12 (0.21)[a]	62.54 (0.28)	67.54 (0.46)
TiO_2	1.50 (0.07)	0.70 (0.05)	0.77 (0.06)
Al_2O_3	16.11 (0.19)	16.74 (0.23)	15.74 (0.21)
FeO[b]	10.84 (0.18)	5.55 (0.06)	4.28 (0.18)
MnO	0.20 (0.04)	0.10 (0.04)	0.12 (0.03)
MgO	7.60 (0.10)	2.97 (0.07)	1.43 (0.06)
CaO	13.32 (0.18)	6.48 (0.12)	4.40 (0.15)
Na_2O	3.56 (0.06)	3.20 (0.05)	3.58 (0.08)
K_2O	0.76 (0.04)	1.69 (0.04)	2.15 (0.07)
Total[c]	100	100	100
Water (wt.%)	1.1	0.7	1.0
NBO/T[d]	0.88	0.25	0.14

[a] Values in parentheses represent one standard deviation.
[b] FeO as total iron.
[c] Recalculated to 100%.
[d] NBO/T values for anhydrous composition were calculated according to Jaeger and Drake (2000). All the iron was assumed to be FeO.

The chemical compositions of andesitic and dacitic glasses were analyzed with an electron microprobe as well as the basaltic glass (Table 1). The water contents in the doubly polished andesitic and dacitic glasses were also determined by IR spectra using thickness from LSCM measurements and the molar absorptivities of 68 and 62 L/mol cm, respectively (Yamashita et al., 1997; Mandeville et al., 2002), to be 0.7 and 1.0 wt.%. The chemical compositions and the water contents of the synthesized glasses are passably homogeneous. These andesitic and dacitic glasses are also used as starting materials for dehydration experiments.

2.2. Dehydration experiments

Dehydration experiments at 400–675 °C were conducted using a Linkam TH-1500MH heating stage, and the water contents of the samples were monitored by FT-IR microspectrometer (Jasco IRT30 + FTIR-620 Plus and MFT-2000). Doubly polished thin sections of the glass samples were used as starting materials. Typical size of the thin sections is 1.5×1.5 mm and the thickness is 24–70 μm (Table 2).

The experimental procedures follow those of Okumura and Nakashima (2004) and are briefly summarized below. First, the temperature of the heating stage was elevated at a rate of 50 °C/min and held at a desired temperature. Second, at the desired temperature a reflectance spectrum of the Pt foil on the heating stage was obtained by FT-IR microspectrometer as a background spectrum. Finally, a sample thin section was put on the Pt foil on the heating stage and sample measurement by FT-IR microspectrometer was started just after the sample setting. The sample measurements were carried out using transmission–reflection technique in which the IR light reflected by the Pt foil was collected.

Table 2
Diffusivity data obtained in this study

	Temperature (°C)	Thickness (μm)	Time (s)	$D_{out,\ const.}$ ($\mu m^2/s$)	$Abs_{0,\ const.}$	$D_{0,\ linear}$ ($\mu m^2/s$)	$Abs_{0,\ linear}$	Remarks[a]
Basalt	400	33	7240	0.00002	131.6	0.00006	131.5	IRT-30
	425	37	18,060	0.00014	122.3	0.00041	122.3	MFT-2000
	450	37	7240	0.00021	158.2	0.00059	158.2	IRT-30
	475	37	18,060	0.00077	117.0	0.00223	117.0	MFT-2000
	500	35	7240	0.00094	145.4	0.00273	145.4	IRT-30
	525	40	18,060	0.00237	135.8	0.00686	144.6	MFT-2000
	550	35	7240	0.00432	130.5	0.01252	130.6	IRT-30
	550	40	18,060	0.00291	153.4	0.00850	153.6	MFT-2000
	565	40	14,340	0.01078, 0.01311[b]	130.3, 136.2[b]	0.03817	136.0	MFT-2000
	575	40	10,910	0.01997, 0.02349[b]	148.7, 157.0[b]	0.08213	162.1	MFT-2000
Andesite	500	65	7260	0.00009	171.8			MFT-2000
	550	46	7240	0.00059	93.3			IRT-30
	575	44	18,060	0.00057	100.0			MFT-2000
	600	67	7260	0.00166	166.9			MFT-2000
	625	44	18,060	0.00141	99.9			MFT-2000
	650	70	7260	0.00330	168.8			MFT-2000
	665	53	25,260	0.00411	102.4			MFT-2000
	665	24	18,060	0.00503	50.7			MFT-2000
	675	53	36,060	0.00651	103.8			MFT-2000
Dacite	500	58	7240	0.00028	161.5	0.00082	161.5	IRT-30
	525	53	18,060	0.00083	186.8	0.00240	186.8	MFT-2000
	550	53	7240	0.00156	140.2	0.00451	140.2	IRT-30
	575	35	18,060	0.00206	185.0	0.00602	185.5	MFT-2000
	600	58	7240	0.00437	160.7	0.01260	160.7	IRT-30
	625	39	18,060	0.00592	110.4	0.01902	112.5	MFT-2000
	650	35	7240	0.00784	102.4	0.02352	103.0	IRT-30
	665	45	18,060	0.01100, 0.01469[b]	111.9, 119.1[b]	0.03990	117.8	MFT-2000
	675	45	11,000	0.01552, 0.02163[b]	121.5, 130.2[b]	0.05456	127.0	MFT-2000

[a] FT-IR microspectrometer used in the in situ dehydration experiments.
[b] Fitting results for the experimental data of $Abs/Abs_0 > 0.5$.

It should be noted that the IR light passes through the sample thin section twice. An IR spectrum was obtained by averaging spectra of 50 scans and the sample measurement was repeated at a 90-s interval during 7240 to 36,060 s using an interval measurement program. Since 50 scans took 40 s by IRT-30 and 60 s by MFT-2000, the IR spectra represent the average for 40 and 60 s. All the spectra in this study were obtained by the aperture size of 100×100 μm.

All the thin sections after the dehydration experiments were observed under an optical microscope. Some bubbles were observed in the thin sections heated at ≥600 °C for basalt and ≥700 °C for andesite. Because the bubble formation causes an uncertainty for determining water diffusivity in the following section, only the experimental results without the bubble formation are reported here. On the other hand, no crystals were found under an optical microscope. Some of the thin sections after the dehydration experiments were observed under JEOL-JXA-8800 electron microprobe, and the chemical compositions of the thin sections were also measured. The chemical compositions of the samples after the dehydration experiments are consistent with those before the dehydration experiment within the uncertainty. Therefore, we conclude that the crystallization during the dehydration experiments was not effective in determining water diffusivity.

3. Results

Successive high temperature IR spectra of basalt, andesite and dacite are shown in Fig. 1. We obtained 81 to 401 IR spectra in a series of a dehydration experiment at a given temperature. The absorption band around 3550 cm^{-1} is attributed to fundamental OH stretching vibration (Stolper, 1982). The intensity of this band corresponds to the sum of the contents of hydroxyl groups and molecular water (e.g., Stolper, 1982). The intensity of the 3550 cm^{-1} band decreased with time, which indicated that total water contents decrease during the dehydration experiment. To describe quantitatively the decrease in the water contents,

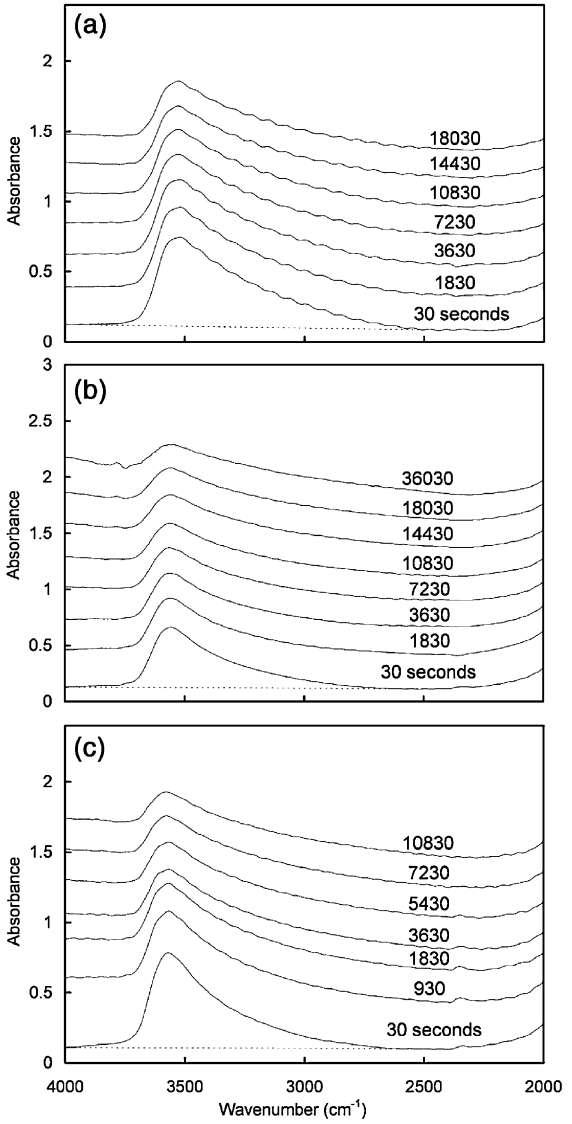

Fig. 1. High temperature infrared (IR) spectra of (a) basalt at 500 °C, (b) andesite at 675 °C and (c) dacite at 675 °C. The numbers in the figure represent the times at which the spectra were obtained. The straight baselines are shown as dotted lines.

we measured integral intensity from 2500 to 4000 cm^{-1} after a straight baseline correction. Because the integral intensity was determined by integrating the peak height with the error of 0.001 from 2500 to 4000 cm^{-1}, the uncertainty of the integral intensity is estimated to be 1.5 cm^{-1}. Initial integral intensities obtained in the experiments were assumed to be a first value obtained at 20 or 30 s after starting the dehydration experiments, because an IR measurement with 50 scans took about 40 and 60 s for IRT-30 and MFT-2000, respectively, and the results were considered to represent the average during the measurement.

The temporal changes in the integral intensities are shown as a function of square root of time divided by sample thickness ($\sqrt{t}/L$) in Fig. 2 which clearly shows that the integral intensities decrease with time and the decrease rate is larger at higher temperature.

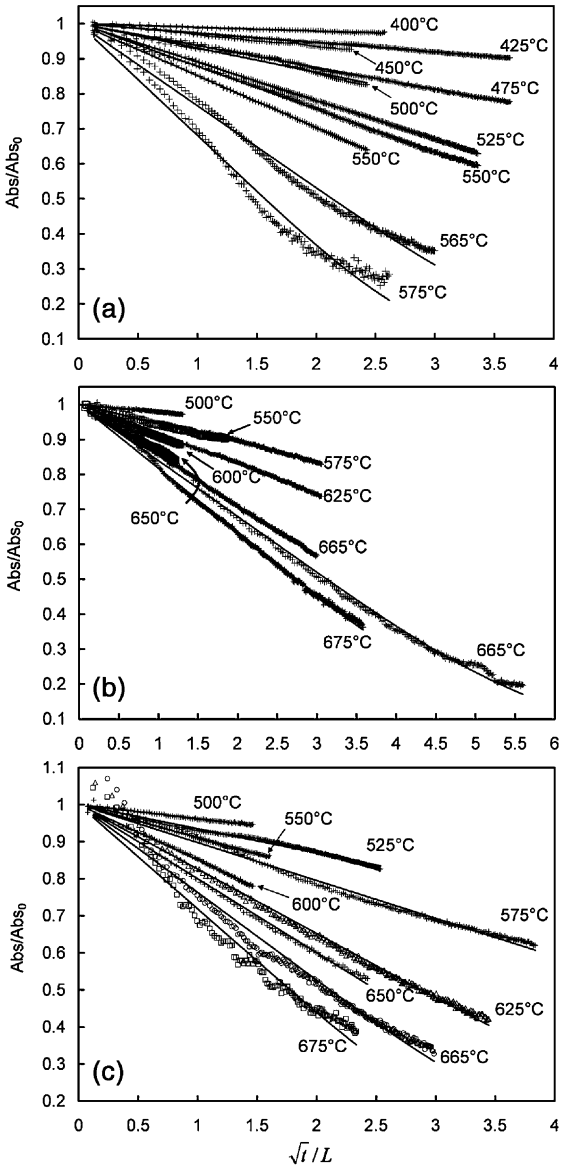

Fig. 2. Integral intensities of IR absorption band for water from 2500 to 4000 cm^{-1} normalized by initial integral intensities (Abs/Abs_0) as a function of square root of time normalized by the sample thickness ($\sqrt{t}/L$) for (a) basalt, (b) andesite and (c) dacite. Initial integral intensities (Abs_0) are determined by fitting Eq. (1) on the experimental data (Table 2). The solid curves represent the fitting results by the diffusion model with the constant diffusivity given by Eq. (1).

4. Discussion

4.1. Determination of water diffusivity

The diffusivities of total water are determined from temporal changes in the integral intensity at 3550 cm^{-1} of sample thin sections. In the following determination of the diffusivity, the sample thin sections (24–70 μm in thickness and 1.5 × 1.5 mm in size) are assumed to be plane sheets (one-dimensional system) and the concentration at sample surface is considered to be zero.

One important issue for the determination of total water diffusivity is how the diffusivity of total water varies with the total water content at a given temperature. When the diffusivity of total water does not depend on the water content, the rate of diffusive water loss from the plane sheet is roughly proportional to the square root of time and the diffusion-out diffusivity can be determined from the following equation (Crank, 1975):

$$M_t = M_0 - M_0\sqrt{\frac{16D_{out}t}{\pi L^2}} \times \left[1 + 2\sqrt{\pi}\sum_{n=1}^{\infty}(-1)^n ierfc\frac{nL}{2\sqrt{D_{out}t}}\right], \quad (1)$$

where M_t is the residual amount of water in the sample, M_0 is the initial amount of water in the sample, D_{out} is the diffusion-out diffusivity, t is the time, and L is the sample thickness. On the other hand, if the diffusivity of total water depends on total water content, Eq. (1) does not hold and the M_t vs. t curve at the concentration-dependent diffusivity is clearly different from that obtained by Eq. (1) (Wang et al., 1996). In this study, we first compare the M_t vs. t curves obtained from the experiments with those calculated from Eq. (1) and determine the diffusion-out diffusivity of total water in basalt to dacite. Eq. (1) well reproduces the experimental data for andesite, but for basalt and dacite the M_t vs. t curves obtained from the experiments clearly differ from those calculated from Eq. (1), which suggest that the total water diffusivity is dependent on total water content. Therefore, we then fit the experimental data by assuming concentration-dependent diffusivity.

4.1.1. Diffusion-out diffusivity

First the experimental data are fitted by Eq. (1) (Fig. 2). In our case, M_t and M_0 in Eq. (1) corresponds to Abs and Abs_0, respectively, where Abs is the integral intensity from 2500 to 4000 cm^{-1} after t in a series of experiments and Abs_0 is the integral intensity at initial condition. The Abs_0 values can not be directly obtained from the experiments, because the sample starts to be dehydrated just after the sample was set at the heating stage. Thus, we consider the Abs_0 values as the unknown parameter as well as the diffusion-out diffusivity D_{out}. In Fig. 2, all the experimental data and the fitting results are shown as the Abs/Abs_0 vs. $\sqrt{t}/L$ plots. The obtained Abs_0 and D_{out} values are listed in Table 2.

For basalt, Eq. (1) successfully reproduces experimental data with small amounts of diffusive water loss ($Abs/Abs_0 > 0.5$) (Fig. 2a). On the other hand, some of the experimental data with large amounts of diffusive loss at 565 and 575 °C (SA565 and SA575) show deviations from the curves predicted by Eq. (1) with increasing amount of diffusive loss. If we fit only the parts of $Abs/Abs_0 > 0.5$ by Eq. (1) for the SA565 and SA575 data, the rates of diffusive loss become slower than those predicted by Eq. (1) with increasing amount of diffusive loss (Fig. 3a). Because Eq. (1) holds at constant diffusivity, the slower rates of diffusive loss

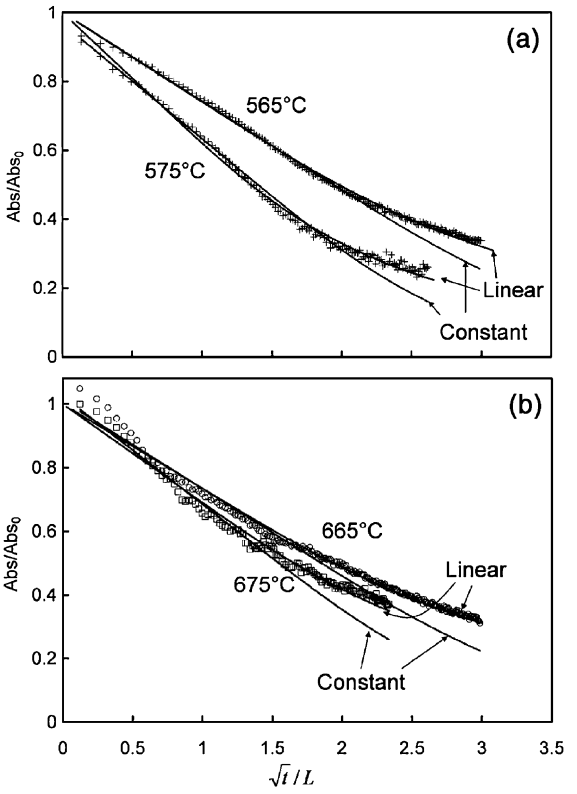

Fig. 3. Normalized integral intensities of IR absorption band for water (Abs/Abs_0) as a function of square root of time normalized by the sample thickness ($\sqrt{t}/L$) for (a) basalt at 565 and 575 °C and (b) dacite at 665 and 675 °C. Initial integral intensities (Abs_0) are obtained by the diffusion model with the linear-dependent diffusivity (Table 2). The solid curves represent the results of the fitting by the diffusion model with the constant diffusivity for the experimental data of $Abs/Abs_0 > 0.5$ (constant) and by the diffusion model with the linear-dependent diffusivity for all the experimental data (linear).

than those predicted by Eq. (1) imply that the diffusivity of total water in basalt decreases with total water contents. The similar trends are also found for dacite at 665 and 675 °C (TPA665 and TPA675) as shown in Figs. 2c and 3b. This result indicates that the diffusivity of total water in dacite is also dependent on total water contents. Therefore, we fit the experimental data for basalt and dacite by assuming concentration-dependent diffusivity in the Following section.

On the other hand, the experimental data for andesite are well fitted by Eq. (1) (Fig. 2b). The experimental data at 665 °C with large amounts of diffusive loss show slight deviations from the curve predicted by Eq. (1), but the deviations are much smaller than those of basalt and dacite. This result indicates that the diffusivity of total water is weakly dependent on or independent of total water contents. Therefore, we assume for andesite that the D_{out} values determined here correspond to total water diffusivity in andesite.

4.1.2. Concentration-dependent diffusivity

To determine concentration-dependent diffusivity of total water in basalt and dacite, the experimental data are numerically fitted by using a functional relationship between the diffusivity and total water contents. In this study, we simply assume the linear dependence of total water diffusivity on total water contents:

$$D = D_0 \frac{[water]}{[water]_0}, \tag{2}$$

where D is the total water diffusivity, D_0 is the diffusivity at the initial water content $[water]_0$, and [water] is the total water contents. This linear dependence is expected from theoretical point of view at low water contents (e.g., Zhang et al., 1991b; Doremus, 1995) and was verified by Liu et al. (2004) for dacite with <0.8 wt.% total water at the temperature ranges of this study. Although the verification of the linear dependence has not been performed for the diffusivity of total water in basalt and dacite with ~1.0 wt.% total water, the linear dependence seems to be appropriate for basalt and dacite in the temperature and water content ranges of this study, because the experimental data are well reproduced by assuming the linear dependence as shown below. Therefore, we determine the diffusivity of total water in basalt and dacite by assuming the linear-dependent diffusivity described as Eq. (2).

In order to extract the diffusivity of total water from the experimental data, we solved numerically the following diffusion equation with the diffusivity given by Eq. (2) and a boundary condition of zero water concentration:

$$\frac{\partial [water]}{\partial t} = \frac{\partial}{\partial x}\left(D \frac{\partial [water]}{\partial x}\right). \tag{3}$$

The numerical calculation was performed as follows. First the profiles of the normalized water content ([water]/$[water]_0$) in the samples were calculated by making $D_0 t/L^2$ (τ), x/L (ξ) and [water]/$[water]_0$ (N) where L is the sample thickness. By combining Eqs. (2) and (3) and using the new variables (τ, ξ and N), the diffusion equation can be transformed to the following equation:

$$\frac{\partial N}{\partial \tau} = \frac{\partial}{\partial \xi}\left(N \frac{\partial N}{\partial \xi}\right). \tag{4}$$

Based on this equation, time evolution of the profile of [water]/$[water]_0$ (N) was calculated by using a time interval of $\Delta\tau$ and diffusion time $j\Delta\tau$ where j is an integer. The profile of N at new time step $j+1$ was then calculated from the N profile at time step j using a forward time center space method. After the calculated N profiles in the plane sheet were integrated using Simpson's Rule, the temporal changes of the integrated values were compared with the experimental data to obtain the best-fit D_0 values. In the fitting procedures, the Abs_0 value was considered as an unknown parameter as well as the D_0 value, and the best-fit values for two unknown parameters (D_0 and Abs_0) were determined by minimizing residual sum of squares for experimental and calculated values.

In this study, the fitting procedures above were applied to all the experimental data for basalt and dacite, although the failure to fit the experimental Abs/Abs_0 vs. $\sqrt{t}/L$ curve by Eq. (1) were found for only the experimental data at higher temperatures (SA565, SA575, TPA665, and TPA675). All the fitting results are shown in Fig. 4 and the obtained Abs_0 and D_0 values are listed in Table 2. All the experimental data for basalt and dacite are well reproduced by assuming the linear dependence of total water diffusivity on total water contents. The obtained D_0 values and the diffusion-out diffusivity D_{out} for basalt and dacite can be expressed as $D_{out} = 0.35 \pm 0.02\ D_0$ which is consistent with the relationship between the D_0 and D_{out} values previously reported by Zhang (1999).

4.1.3. Diffusivity of total water in basalt, andesite and dacite at 400–675 °C

The results of this study show that the diffusivities of total water in basalt and dacite are dependent on total

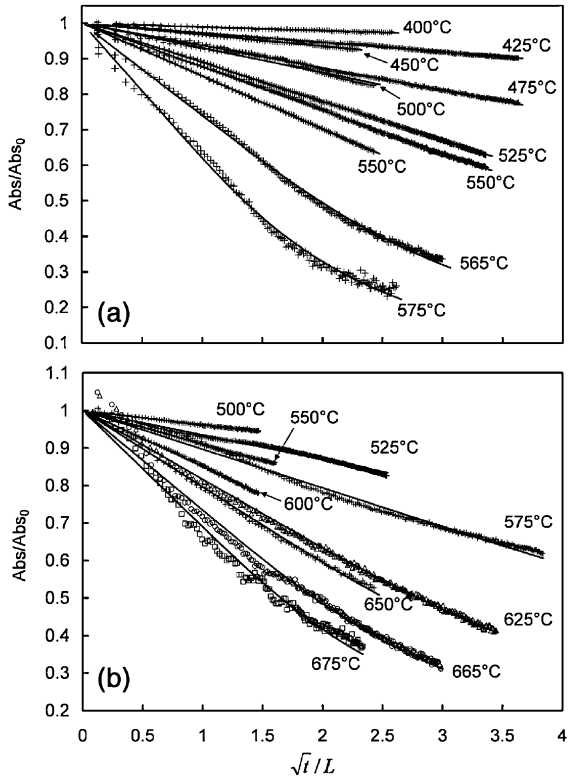

Fig. 4. Normalized integral intensities of IR absorption band for water (Abs/Abs_0) as a function of square root of time normalized by the sample thickness ($\sqrt{t}/L$) for (a) basalt and (b) dacite. Initial integral intensities (Abs_0) are obtained by the diffusion model with the linear-dependent diffusivity. The solid curves represent the results of the fitting by the diffusion model with the linear-dependent diffusivity.

water contents, and the obtained D_0 values are expressed by the following Arrhenius relations (Fig. 5):

$$\ln D_{0,\mathrm{Basalt}} = (20.2\pm2.1) - (166,000\pm13,000)/RT \quad (5a)$$

$$\ln D_{0,\mathrm{Dacite}} = (13.9\pm0.9) - (133,000\pm6000)/RT \quad (5b)$$

These equations reproduce experimental results within the averaged and maximum errors of 0.18 and 0.35 log units for basalt and 0.06 and 0.11 log units for dacite. Combining Eqs. (5a) and (5b) with Eq. (2), the diffusivities of total water in basalt and dacite are described as

$$D_{\mathrm{Basalt}} = C/C_0\exp[(20.2\pm2.1) - (166,000\pm13,000)/RT] \quad (6a)$$

$$D_{\mathrm{Dacite}} = C/C_0\exp[(13.9\pm0.9) - (133,000\pm6000)/RT], \quad (6b)$$

where C_0 is 1.1 and 1.0 wt.% for basalt and dacite, respectively. These diffusivities of total water cover the temperature ranges of 400–575 °C for basalt and 500–675 °C for dacite, respectively.

On the other hand, the experimental data showed that the diffusivity of total water in andesite was weakly dependent on or independent of total water contents. However, the exact functional form of how the diffusivity of total water in andesite depends on total water contents is unclear yet, because this study did not investigate the diffusion profile but the dehydration rates. Therefore additional studies seem to be necessary to clarify the exact functional form. When the diffusivity in andesite is assumed to be the constant value, the diffusivity can be described as a function of temperature (Fig. 5):

$$D_{\mathrm{Andesite}} = \exp[(12.4\pm1.4) - (138,000\pm10,000)/RT] \quad (6c)$$

This expression for andesite reproduces the experimental results within the averaged and maximum errors of 0.09 and 0.19 log units, and covers only the temperature ranges of 500 to 675 °C. We do not recommend that these expressions for the diffusivity of total water are applied to the estimation of the diffusivities at the water contents of more than 1.1, 0.7 and 1.0 wt.% for basalt, andesite and dacite, respectively, because the dependences of total water diffusivity on total water contents at higher water contents possibly differ from those at lower water content ranges of this study. For example, it has been reported that the diffusivity of total water rapidly increases at more than 2 wt.% for rhyolite (Zhang, 1999).

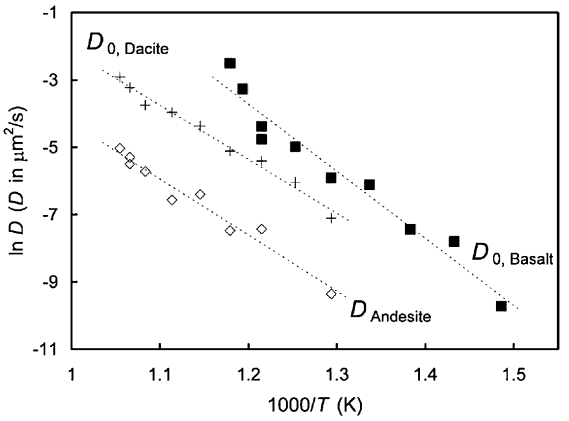

Fig. 5. The D_0 values for basalt ($D_{0,\mathrm{Basalt}}$) and dacite ($D_{0,\mathrm{Dacite}}$) and the diffusivity of total water in andesite (D_{Andesite}) are shown as a function of temperature. The linear regressions for the experimental results (dotted lines) provide the Arrhenius relations represented by Eqs. (5a),(5b) and (6c) for basalt, dacite and andesite, respectively.

4.2. Effect of silicate composition on water diffusion

The diffusivities of total water at 0.7 wt.% water calculated from Eqs. (6a) (6b) and (6c) are shown in Fig. 6 as a function of temperature to compare the water diffusivity in basalt to rhyolite. The diffusivity of total water in rhyolite shown in Fig. 6 is data from Zhang and Behrens (2000) which covers wide water content and temperature ranges. At 400–675 °C, the diffusion of total water in rhyolite is the fastest and that in andesite is the slowest among basaltic to rhyolitic compositions (Fig. 6). The diffusivity in andesite is smaller than that in rhyolite by more than one order of magnitude (0.05 $\mu m^2/s$ in rhyolite and 0.001 $\mu m^2/s$ in andesite at 600 °C).

To present quantitatively the dependence of total water diffusivity on anhydrous silicate compositions, the pre-exponential factor D_f and the activation energy E_a obtained from Arrhenius relation $D=D_f \exp(-E_a/RT)$ at 0.7 wt.% water content are plotted as a function of the ratio of non-bridging oxygen to tetrahedrally coordinated cation (NBO/T) (Fig. 7a,b). The pre-exponential factor and the activation energy for water diffusion in rhyolite calculated from the data by Zhang and Behrens (2000) are also plotted in Fig. 7. Although the quantitative description of multicomponent silicate structure is difficult due to the presence of many components, an essence for the description of the silicate structure seems to be the polymerization degree. The viscosity of silicate melts directly linked to the silicate structure is dependent on the polymerization degree (e.g., Giordano and Dingwell, 2003). Therefore, this study considers the dependence of water diffusivity on anhydrous silicate composition using NBO/T as a primary measure. The ln D_f vs. NBO/T and E_a vs. NBO/T relationships in Fig. 7a,b show that the pre-exponential factor and the activation energy roughly increase with NBO/T. A physical meaning of the pre-exponential factor is the diffusive jump distance, and the activation energy corresponds to the energy barrier to diffuse from one pore to another (e.g., Lasaga, 1981a; Chakraborty, 1995). Thus, the increases of the pre-ex-

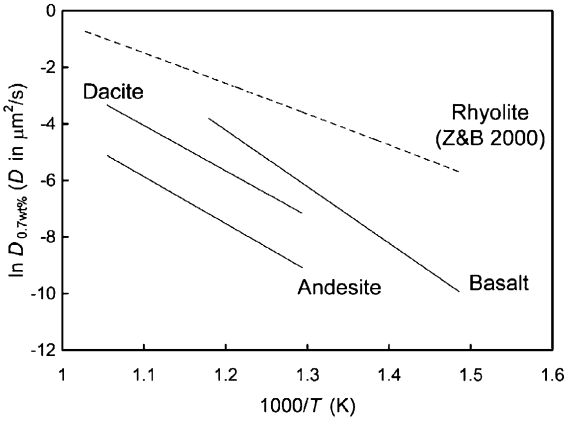

Fig. 6. Diffusivities of total water in basalt, andesite and dacite at 0.7 wt.% total water and 0.1 MPa, calculated from Eqs. (6a–c), respectively. The data for rhyolite (dotted line) are calculated from the result of Zhang and Behrens (2000) (Z&B 2000).

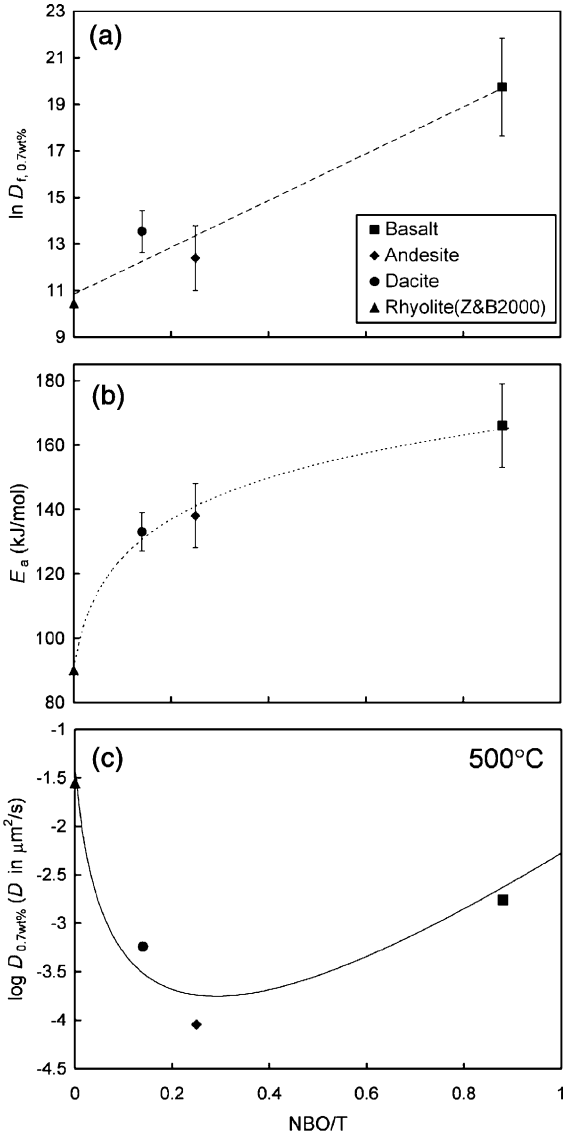

Fig. 7. (a) Pre-exponential factor D_f, (b) activation energy E_a in Arrhenius relation for water diffusion and (c) total water diffusivity obtained from the experiments and calculated from Eq. (8) at 0.7 wt.% water are plotted as a function of NBO/T (listed in Table 1). The error bars represent one standard deviation. The dotted curves represent the regression for experimental data; (a) ln $D_{f,\ 0.7\ wt.\%}=10.82+10.0$ NBO/T and (b) $E_a=167{,}000+20{,}000$ ln[NBO/T+0.021]. The solid line represents the diffusivity estimated from Eq. (8).

ponential factor and the activation energy imply the increases of the jump distance and energy barrier with NBO/T. With the depolymerization (increase in NBO/T), the jump distance might increase due to the occupation of neighboring pore space by the larger alkaline and alkaline earth elements than the network formers (Si and Al). With this occupation of neighboring pore space by larger cations, the energy barrier for water diffusion also increases, because the energy barrier is directly related to the gate width in silicate structure through that water has to pass (e.g., Jambon, 1982).

The empirical relation between D_f and E_a has been known as a "compensation law" ($E_a = a + b \log D_f$ where a and b are the constants) (e.g., Lasaga, 1981b), and is expressed as $E_a = (36 \pm 37) + (16 \pm 6) \log D_f$ for the diffusivity of total water obtained in this study. This relation may be useful to describe the dependence of D_f and E_a on anhydrous silicate composition. However, the empirical relation based on the compensation law produces large uncertainties for the results of this study. Therefore, we fitted empirically the relation of ln D_f vs. NBO/T and E_a vs. NBO/T (Fig. 7a,b) by linear and logarithmic functions as follows:

$$\ln D_{f,0.7\ \mathrm{wt.\%}} = (10.82 \pm 0.79) + (10.0 \pm 1.7)\mathrm{NBO/T} \quad (7a)$$

$$E_a = (167,000 \pm 4000) + (20,000 \pm 4000)\ln[\mathrm{NBO/T} + (0.021 \pm 0.014)], \quad (7b)$$

where D_f is the pre-exponential factor in $\mu m^2/s$ and E_a is the activation energy in J/mol. By combining Eqs. (7a) and (7b) with Arrhenius relation, the following empirical formulation is derived to estimate the total water diffusivity D at 0.7 wt.%, 400–675 °C and 0.1 MPa:

$$D_{0.7\ \mathrm{wt.\%}} = \exp\left[10.82 + 10.0\mathrm{NBO/T} - \left(\frac{167,000 + 20,000\ln(\mathrm{NBO/T} + 0.021)}{RT}\right)\right]. \quad (8)$$

This expression reproduces the experimental (8) data obtained in this study within the averaged and maximum errors of 0.27 and 0.48 log units, and the diffusivity of total water in rhyolite calculated from Eq. (8) is consistent with that estimated from the results of Zhang and Behrens (2000) within 0.20 log units. We show the diffusivity at 500 °C calculated from Eq. (8) as a function of NBO/T in Fig. 7c. The variation of the diffusivity with the change in NBO/T is well reproduced by Eq. (8), i.e. decrease of the diffusivity with increasing NBO/T at low NBO/T value (NBO/T = 0–0.2) and increase of the diffusivity with increasing NBO/T at high NBO/T value.

As a first approximation, we described the compositional dependence of total water diffusivity by using NBO/T. However, the description of the diffusivity in natural silicate glasses and melts seems to be not so simple, because all chemical components have different roles in silicate structures. For example, hydrogen diffusion possibly plays a role for the transport of water species in basalt and andesite with higher iron content due to redox reaction of $2FeO + H_2O = Fe_2O_3 + H_2$, although the diffusive water species is considered as molecular water in dacite and rhyolite (Zhang et al., 1991a,b; Behrens and Nowak, 1997; Liu et al., 2004). Hence, additional investigation of water diffusion in natural and controlled composition glasses and melts will be needed to resolve and describe quantitatively the compositional dependence of water diffusion.

4.3. Comparison with previous studies

This study investigated the diffusivities of total water in basalt, andesite and dacite at lower temperatures and pressure than those of previous studies. We compare the diffusivity determined in this study with available previous data by extrapolating the diffusivity

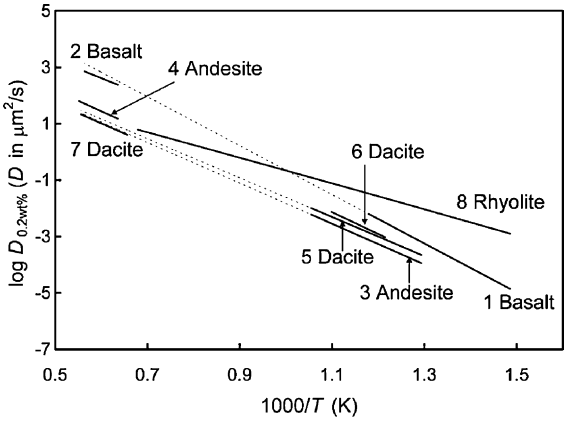

Fig. 8. Summary of total water diffusivity in basalt to rhyolite at 0.2 wt.% water. The solid lines represent the diffusivities obtained in this study (1 basalt, 3 andesite, 5 dacite), Zhang and Stolper (1991) (2 basalt), Behrens et al. (2004) (4 andesite, 7 dacite), Liu et al. (2004) (6 dacite) and Zhang and Behrens (2000) (8 rhyolite). The dotted lines represent the diffusivities estimated by extrapolations from those at 400–675 °C to higher temperatures.

to higher temperatures based on the Arrhenius relation (Fig. 8).

First the diffusivity of total water in basalt at 400–575 °C and 0.2 wt.% is extrapolated to higher temperatures to compare with the results of Zhang and Stolper (1991) which determined the diffusivity of total water in basaltic melts with <0.43 wt.% water at 1300–1500 °C and 1.0 GPa. The diffusivities at 0.2 wt.% total water calculated from the results of this study and data from Zhang and Stolper (1991) are shown as lines 1 and 2 in Fig. 8, respectively. When the diffusivity at higher temperatures is estimated by extrapolating the diffusivity of this study based on the activation energy of 166 kJ/mol (dotted line in Fig. 8), the water diffusivity is consistent with that of Zhang and Stolper (1991) within the error of 0.29 log units. The diffusivity estimated by the extrapolation is slightly larger than that of Zhang and Stolper (1991), which might indicate that the diffusivity of total water in basalt decreases with increasing pressure, because the diffusivity was determined at 0.1 MPa in this study and 1.0 GPa in Zhang and Stolper (1991).

Second the total water diffusivity in andesite at 500–675 °C is extrapolated to higher temperatures to compare with the results reported by Behrens et al. (2004) (lines 3 and 4 in Fig. 8). The extrapolated values are lower than the total water diffusivity of Behrens et al. (2004). For example, the diffusivity at 1300 °C and 0.2 wt.% is estimated to be 6 and 15 $\mu m^2/s$ by the extrapolation of the result of this study and the result of Behrens et al. (2004), respectively. A source of this difference is the difference of how the diffusivity of total water depends on total water contents at lower temperatures and higher temperatures. We showed that the diffusivity of total water in andesite was weakly dependent on or independent of total water contents at around 675 °C. Behrens et al. (2004) reported that the diffusivity of total water in andesite was roughly proportional to total water contents at higher temperatures (1135–1621 °C) in the range of 0.1–0.4 wt.% total water. To model the diffusion of water in andesite at wider temperature ranges and to reveal the mechanism of water diffusion in andesite, it will be necessary to investigate how the diffusivity of total water in andesite depends on total water contents at intermediate temperatures, i.e., 700–1100 °C. Another source of the difference might be the positive pressure dependence of total water diffusivity in andesite. In fact, Behrens et al. (2004) have found the dependence of the water diffusivity on pressure for the pressure ranges of 0.5–1.5 GPa.

Finally the diffusivity of total water in dacite at 500–675 °C and 0.2 wt.% total water is extrapolated to higher temperatures to compare with the result reported by Behrens et al. (2004) (lines 5 and 7 in Fig. 8). For dacite, the water diffusivity estimated from our results is similar to the water diffusivity by Behrens et al. (2004). The slight difference might indicate that the diffusivity of total water in dacite decreases with increasing pressure as well as total water diffusivity in basalt. The diffusivity estimated from the result of this study is similar to the results of Liu et al. (2004) (line 6 in Fig. 8) which determined the diffusivity of total water in dacite at 550–640 °C and <150 MPa. For example, the diffusivities in dacite calculated from the results of this study and Liu et al. (2004) are 0.0023 and 0.0032 $\mu m^2/s$ at 600 °C, respectively.

The diffusivity of total water in natural composition glasses and melts is strongly dependent on anhydrous silicate composition as shown in the Previous section. Behrens et al. (2004) reported that the diffusivity of total water in silicate melts increases with melt depolymerization at temperatures above 1200 °C. Although the diffusivity at lower temperatures determined in this study can not be simply related to the polymerization degree, the extrapolation of the diffusivity from 400–675 °C to higher temperatures suggests that the diffusivity increases with depolymerization, which results in crossover of diffusivity–temperature trends (Fig. 8), as reported by Behrens et al. (2004).

5. Conclusions

Dehydration experiments for basaltic, andesitic and dacitic glasses with 1.1, 0.7 and 1.0 wt.% water were carried out at 400–675 °C in order to determine the diffusivities of total water. The dehydration rates of the samples were monitored under FT-IR microspectrometer. The results of the dehydration experiments showed that the diffusivities of total water in basalt and dacite were linearly dependent on total water contents, but that in andesite was weakly dependent on or independent of total water contents. Therefore, the total water diffusivities in basalt and dacite were determined by assuming the linear-dependent diffusivity on total water contents and that in andesite was obtained by assuming the constant diffusivity. The results of this study and previous data for water diffusion in rhyolite indicated that the diffusivity of total water was sensitive to anhydrous silicate composition and that the diffusivity in rhyolite was the largest and that in andesitic glass was the smallest in basaltic to rhyolitic compositions around 500 °C. On the other hand, the extrapolation of the total water diffusivity from 400–675 °C to higher temperatures predicts that the diffusivity increases with

melt depolymerization. To clarify this dependence of total water diffusivity on anhydrous silicate composition, the pre-exponential factor D_f and the activation energy E_a obtained from Arrhenius relation $D=D_f \exp(-E_a/RT)$ were compared with the ratio of non-bridging oxygen to tetrahedrally coordinated cation (NBO/T) of the studied glasses. This showed that ln D_f and E_a increased with increasing NBO/T from rhyolite to basalt. These dependences of ln D_f and E_a on anhydrous composition may be understood by the following model. With introducing alkaline and alkaline earth elements from rhyolite to basalt, the diffusive jump distance increases due to the occupation of neighboring pore spaces by the larger alkaline and alkaline earth elements than the network formers (Si and Al). This occupation of neighboring pore spaces by larger cations also increases the energy barrier for water diffusion, because this energy barrier is related to the gate width in silicate structure for water diffusion. Further systematic measurements of water diffusivity in natural and controlled composition glasses and melts will be needed to resolve and describe quantitatively the complex behavior of water diffusion.

Acknowledgements

We would like to thank S. Takeuchi for EPMA analyses and for providing the pumice from the 1914 eruption at Sakurajima Volcano. We also thank K. Ishihara and M. Iguchi for providing the pumice from the 1975 eruption at Sakurajima Volcano and E. Takahashi and N. Hirano for providing basaltic glass obtained at 250 km southern sea floor from Hawaii Island during the 697th dive of the JAMSTEC (Japan Marine Science and Technology Center) submersible *Shinkai 6500* on 2001. We would like to thank E. Takahashi, T. Suzuki and A. Tomiya for their helpful support in the high *P–T* experiments. The constructive comments by M. Ikoma and M. Yamaguchi greatly helped the numerical calculations. We thank Y. Zhang and an anonymous reviewer for constructive reviews. This research was supported by Research Fellowships of the Japan Society for the Promotion of Science for Young Scientists to S.O., and funded by Grand-in-Aid for scientific research (422-A02-14080202) to S.N. **[RR]**

References

Behrens, H., Nowak, M., 1997. The mechanisms of water diffusion in polymerized silicate melts. Contrib. Mineral. Petrol. 126, 377–385.

Behrens, H., Zhang, Y., 2001. Ar diffusion in hydrous silicic melts: implications for volatile diffusion mechanisms and fractionation. Earth Planet. Sci. Lett. 192, 363–376.

Behrens, H., Zhang, Y., Xu, Z., 2004. H_2O diffusion in dacitic and andesitic melts. Geochim. Cosmochim. Acta 68, 5139–5150.

Chakraborty, S., 1995. Diffusion in silicate melts. In: Stebbins, J.F., McMillan, P.F., Dingwell, D.B. (eds), Structure, Dynamics and Properties of Silicate Melts vol. 32. Mineralogical Society of America, Washington, DC, pp. 411–503.

Crank, J., 1975. The Mathematics of Diffusion. Clarendon Press, Oxford.

Delaney, J.R., Karsten, J.L., 1981. Ion microprobe studies of water in silicate melts. Concentration-dependent water diffusion in obsidian. Earth Planet. Sci. Lett. 52, 191–202.

Doremus, R.H., 1995. Diffusion of water in silica glass. J. Mater. Res. 10, 2379–2389.

Giordano, D., Dingwell, D.B., 2003. Non-Arrhenian multicomponent melt viscosity: A model. Earth Planet. Sci. Lett. 208, 337–349.

Hess, K.-U., Dingwell, D.B., 1996. Viscosities of hydrous leucogranitic melts: a non-Arrhenian model. Am. Mineral. 81, 1297–1300.

Jaeger, W.L., Drake, M.J., 2000. Metal-silicate partitioning of Co, Ga, and W: dependence on silicate melt composition. Geochim. Cosmochim. Acta 22, 3887–3895.

Jambon, A., 1982. Tracer diffusion in granitic melts: experimental results for Na, Ka, Rb, Cs, Ca, Sr, Ba, Ce, Eu, to 1300 °C and a model of calculation. J. Geophys. Res. 87, 10797–10810.

Jambon, A., Zhang, Y., Stolper, E.M., 1992. Experimental dehydration of natural obsidian and estimation of D_{H_2O} at low water contents. Geochim. Cosmochim. Acta 56, 2931–2935.

Karsten, J.L., Holloway, J.R., Delaney, J.R., 1982. Ion microprobe studies of water in silicate melts: temperature-dependent water diffusion in obsidian. Earth Planet. Sci. Lett. 59, 420–428.

Lapham, K.M., Holloway, J.R., Delaney, J.R., 1984. Diffusion of H_2O and D_2O in obsidian at elevated temperatures and pressures. J. Non-Cryst. Solids 67, 179–191.

Lasaga, A.C., 1981a. Transition state theory. In: Lasaga, A.C., Kirkpatrick, R.J. (eds.), Kinetics of Geochemical Processes vol. 8. Mineralogical Society of America, Washington, DC, pp. 135–169.

Lasaga, A.C., 1981b. The atomic basis of kinetics: defects in minerals. In: Lasaga, A.C., Kirkpatrick, R.J. (eds), Kinetics of Geochemical Processes vol. 8. Mineralogical Society of America, Washington, DC, pp. 261–320.

Lensky, N.G., Lyakhovsky, V.L., Navon, O., 2001. Radial variation of melt viscosity around growing bubbles and gas overpressure in vesiculating magmas. Earth Planet. Sci. Lett. 186, 1–6.

Liu, Y., Zhang, Y., 2000. Bubble growth in rhyolitic melt. Earth Planet. Sci. Lett. 181, 251–264.

Liu, Y., Zhang, Y., Behrens, H., 2004. H_2O diffusion in dacitic melts. Chem. Geol. 209, 327–340.

Mandeville, C.W., Webster, J.D., Rutherford, M.J., Taylor, B.E., Timbal, A., Faure, K., 2002. Determination of molar absorptivities for infrared absorption bands of H_2O in andesitic glasses. Am. Mineral. 87, 813–821.

Melnik, O., Sparks, R.S.J., 1999. Nonlinear dynamics of lava dome extrusion. Nature 402, 37–41.

Nowak, M., Behrens, H., 1997. An experimental investigation on diffusion of water in haplogranitic melts. Contrib. Mineral. Petrol. 126, 365–376.

Ochs, F.A., Lange, R.A., 1999. The density of hydrous magmatic liquids. Science 283, 1314–1317.

Okumura, S., Nakashima, S., 2004. Water diffusivity in rhyolitic glasses as determined by in situ IR spectroscopy. Phys. Chem. Miner. 31, 183–189.

Shaw, H.R., 1974. Diffusion of H_2O in granitic liquids: I. Experimental data: II. Mass transfer in magma chambers. In: Hofmann, A.W.,

et al. (eds), Geochemical Transport and Kinetics vol. 634. Carnegie Inst. Washington Publ, pp. 139–170.

Sparks, R.S.J., Barclay, J., Jaupart, C., Mader, H.M., Phillips, J.C., 1994. Physical aspects of magma degassing I. Experimental and theoretical constraints on vesiculation. In: Carroll, M.R., Holloway, J.R. (eds), Volatiles in Magmas vol. 30. Mineralogical Society of America, Washington, DC, pp. 413–445.

Stolper, E.M., 1982. Water in silicate glasses: an infrared spectroscopic study. Contrib. Mineral. Petrol. 81, 1–17.

Toramaru, A., 1995. Numerical study of nucleation and growth of bubbles in viscous magmas. J. Geophys. Res. 100, 1913–1931.

Wang, L., Zhang, Y., Essene, E.J., 1996. Diffusion of the hydrous component in pyrope. Am. Mineral. 81, 706–718.

Yamashita, S., Kitamura, T., Kusakabe, M., 1997. Infrared spectroscopy of hydrous glasses of arc magma compositions. Geochem. J. 31, 169–174.

Zhang, Y., 1999. H_2O in rhyolitic glasses and melts: measurement, speciation, solubility, and diffusion. Rev. Geophys. 37, 493–516.

Zhang, Y., Behrens, H., 2000. H_2O diffusion in rhyolitic melts and glasses. Chem. Geol. 169, 243–262.

Zhang, Y., Stolper, E.M., 1991. Water diffusion in basaltic melt. Nature 351, 306–309.

Zhang, Y., Stolper, E.M., Wasserburg, G.J., 1991a. Diffusion of water in rhyolitic glasses. Geochim. Cosmochim. Acta 55, 441–456.

Zhang, Y., Stolper, E.M., Wasserburg, G.J., 1991b. Diffusion of a multi-species component and its role in oxygen and water transport in silicates. Earth Planet. Sci. Lett. 103, 228–240.